Clinical and Translational Oncology
https://doi.org/10.1007/s12094-024-03592-4

RESEARCH ARTICLE

Poor therapeutic outcomes in KRAS-mutant non-small cell lung cancer due to chemoresistance conferred by SLC7A11

Shiyu Zhang[1] · Yutong Ge[1] · Jingwen Liu[1] · Kaihua Lu[1]

Received: 4 June 2024 / Accepted: 30 June 2024

Abstract

Purpose This study aimed to confirm whether Kirsten rat sarcoma viral oncogene (KRAS) mutations affect the therapeutic efficacy of non-small cell lung cancer (NSCLC) and, if so, to explore what the possible mechanisms might be.

Methods We retrospectively analyzed the efficacy of immunochemotherapy in KRAS-mutant NSCLC patients compared to driver-negative patients. Online data platforms were used to find immunotherapy cases, and survival analysis compared treatments' efficacy. Cytotoxicity assays measured chemosensitivity in KRAS-mutant versus wild-type NSCLC to drugs like paclitaxel, carboplatin, and pemetrexed. Bioinformatics confirmed the KRAS-SLC7A11 link and cell experiments tested SLC7A11's role in chemoresistance. Animal studies verified the antitumor effects of SLC7A11 inhibitors with chemotherapy.

Results Patients with KRAS-mutated NSCLC have a shorter therapeutic effectiveness duration with immunochemotherapy than patients with driver gene-negative status. The efficacy of immunotherapy alone is similar between the two groups. The KRAS mutation can enhance chemoresistance by upregulating SLC7A11, and inhibiting SLC7A11 can increase the sensitivity of KRAS-mutated NSCLC to chemotherapy.

Conclusion This study suggests that KRAS-mutant NSCLC can enhance its acquired chemoresistance by overexpressing SLC7A11, leading to poorer therapeutic outcomes. Targeting the KRAS-SLC7A11 axis could increase sensitivity to chemotherapeutic drugs, providing theoretical support for future treatment directions.

Keywords KRAS · NSCLC · Chemoresistance · Lipid peroxidation · Immunotherapy

Introduction

The Kirsten rat sarcoma viral oncogene (KRAS) mutation is one of the common mutation types in non-small cell lung cancer (NSCLC) [1–3]. We've encountered two advanced NSCLC patients with rapid progression and poor treatment response, both with KRAS mutations, prompting us to investigate the mutation's impact on efficacy. Prognostic values of KRAS in NSCLC are mixed, with some studies showing worse outcomes and others finding no difference [4–7]. While KRAS patients are often treated with immunochemotherapy, its effect on advanced NSCLC efficacy compared to non-mutant patients is unclear [8]. Therefore, we decided to further explore this issue.

The ferroptosis inducers RAS-selective lethal compound 3 (RSL3) and RAS and small T antigen-expressing cells eradicator (Erastin) selectively target RAS-mutant cells. RSL3 induces ferroptosis by inhibiting glutathione peroxidase 4 (GPX4) directly at low doses [9, 10], while Erastin inhibits GPX4 indirectly by targeting SLC7A11, a subunit of the system xc- [11]. Ferroptosis, marked by GSH depletion and GPX4 inactivation, leads to cell death through lipid peroxidation accumulation. Glutathione (GSH), an antioxidant, prevents cell death by reducing lipid peroxidation via GPX4 [4, 11]. The system xc-—GPX4 axis regulates cellular redox balance by controlling GSH levels. Given RSL3 and Erastin's selectivity for RAS mutations, we're exploring if the GSH synthesis pathway is linked to drug resistance in KRAS mutant NSCLC and their potential therapeutic application [7, 12].

✉ Kaihua Lu
13605179453@126.com

[1] Department of Oncology, First Affiliated Hospital with Nanjing Medical University, 300 Guangzhou Road, Nanjing 210029, People's Republic of China

Published online: 26 July 2024

Materials and methods

Retrospective data collection

Data collection was approved by the Ethics Committee of The First Affiliated Hospital with Nanjing Medical University (Approval Number: 2022-SR-357), involved patients from the Oncology Department between August 1, 2022, and December 31, 2023. The KRAS mutation group included patients with advanced or metastatic NSCLC diagnosed via pathology, and confirmed KRAS mutations without other lung cancer driver genes (as defined by the 2024 National Comprehensive Cancer Network Clinical Practice Guidelines in Oncology for NSCLC). The control group comprised patients with advanced NSCLC without driver genes. Treatment efficacy was evaluated using the Response Evaluation Criteria in Solid Tumors Version 1.1 (RECIST 1.1), dividing patients into durable clinical benefit (DCB) (with complete response (CR) or partial response (PR) and stable disease (SD) lasting ≥ 6 months) and no durable benefit (NDB) groups (with progressive disease (PD) and SD < 6 months).

Bioinformatics analysis

We identified lung cancer immunotherapy studies on the cBioPortal FOR CANCER GENOMICS website (https://www.cbioportal.org/), selecting advanced NSCLC cases treated solely with immunotherapy. The KRAS and the control group criteria was same as the retrospective analysis.

Cell experiments

Cell lines

Four NSCLC cell lines (A549, NCI-H23, NCI-H1975, NCI-H1299) were purchased from Procell Life Science & Technology in Wuhan, China. A549 harbors KRAS G12S mutation, H23 harbors KRAS G12C mutation, and both H1975 and H1299 are KRAS wild-type cell lines.

Cell counting kit-8 (CCK8)

Cells were plated uniformly in a 96-well plate at 5000 cells/well with drug-containing medium for 48 h. The CCK8 (Biosharp, China) solution was mixed 1:9 with medium and incubated 1–2 h before measuring absorbance at 450 nm with a Multiskan FC photometer.

Clonogenic assay

Cells were evenly seeded in a 6-well plate (3000 cells/well) with drug-containing medium for 10 days before fixation and staining.

Chemotherapy resistance model

Resistance model: KRAS mutant and wild-type cells were exposed to varying paclitaxel concentrations. CCK8 assessed viability on days 3, 6, and 9 post-exposures. Proliferation rate was the ratio of treated to untreated cell viability; values < 1 suggest drug sensitivity, while > 1 indicate resistance development.

Cross-resistance model: Post-paclitaxel resistance cells were cultured with cisplatin and pemetrexed, and proliferation was measured by CCK8 at 24-, 48-, and 72-h post-removal of paclitaxel.

The same procedures were followed for cisplatin and pemetrexed resistance models and cross-resistance models as for paclitaxel.

Transfection

Small interfering RNA (siRNA, GenePharma, China) Sequences are listed in the Online Resource Table S1. Cells were plated in a 6-well plate at 3×10^5 cells/well and transfected once 60–70% confluent.

Western blotting (WB)

Cells were lysed in RIPA buffer with PMSF at 1:100. Proteins were separated by SDS-PAGE, transferred to PVDF, blocked, and incubated with β-actin, SLC7A11, and KRAS antibodies at 4 °C overnight. Following secondary antibody incubation, membranes were washed and exposed. Protein expression was quantified using ImageJ, and the relative protein expression was normalized to the control group's target protein/β-actin ratio set to 1, with other groups' relative expression levels compared to the control group.

Flow cytometry

Cells were incubated with 5 μM C11 BODIPY 581/591 (GlpBio, USA) for 30 min, washed thrice with phosphate buffered saline (PBS), and prepared in flow cytometry tubes. Analysis was done using a flow cytometer with a

488 nm laser, detecting emissions at 505–550 nm (FL1) and > 580 nm (FL2).

GSH assay

The GSH-GSSG assay kit was from Beyotime (Shanghai, China). Samples and standards were prepared according to the instructions.

Animal experiments

Animal studies were approved (IACUC-2201042) and conducted at Nanjing Medical University. Four-week-old female nude mice, (17 ± 2) g, from GemPharmatech, were housed there. H23 were subcutaneously implanted at 10^6 cells/100 µl PBS. Tumor growth was checked every three days. Mice underwent biweekly intraperitoneal injections of paclitaxel (10 mg/kg), carboplatin (30 mg/kg), pemetrexed (50 mg/kg), and Erastin (30 mg/kg) for 4–6 cycles. They were then euthanized, tumors were excised for analysis, and relative tumor volume was calculated as the ratio of post- to pre-treatment volumes.

Data analysis

Survival was analyzed using the Kaplan–Meier method and Log-rank test. Baseline data were assessed with Cox multivariate analysis and Pearson's for correlations. ImageJ counted colonies and scored immunohistochemistry. Statistical tests included unpaired T-tests, Tukey's, or Chi-square, with $P < 0.05$ for significance. Data are mean ± standard error of the mean (SEM).

Results

Poor efficacy of first-line treatment in KRAS mutant advanced NSCLC

In a retrospective analysis of 1,253 patients, we found 30 with advanced NSCLC and KRAS mutations, and 49 without driver genes. Online Resource Table S2 details clinical characteristics, indicating immunochemotherapy as the primary treatment for both groups.

Figure 1 outlines first-line treatment efficacy, with median progression-free survival (mPFS) at 7.87 months for KRAS mutants and 14.93 months for controls [Fig. 1A: $P < 0.01$, HR 1.88, 95% confidence interval (CI) 0.9673–3.669]. The objective response rates (ORR) was 26.7% for KRAS and 42.9% for controls (Fig. 1B), with disease control rates (DCR) at 86.7% and 93.9%, respectively (Fig. 1C). The KRAS group's DCB rate was 60%, significantly below the control group's 81.6% (Fig. 1D). No significant differences were found in Ki-67, tumor mutation burden (TMB), and PD-L1 expression (Fig. 1E–G). KRAS group mutations primarily included subtypes G12C, G12D, and G12V (Fig. 1H).

Similar immunotherapy efficacy between the KRAS mutant and the driver genes negative population

We identified six immunotherapy-related studies (Online Resource Table S3) and selected a total of 223 cases with KRAS mutations and 316 cases without driver genes. Clinical characteristic was shown in Online Resource Table S4. The mutation subtypes in the KRAS group are shown in Fig. 2A. There was no significant difference in TMB and PD-L1 between the KRAS group and the control group (Fig. 2B, C).

Given KRAS G12C's targetability and potential distinct immunotherapy response, we analyzed G12C patients separately. PFS showed no significant difference between the KRAS group (95 G12C, 128 other KRAS mutations) and controls (Fig. 2D, $P = 0.758$). OS data included 194 KRAS cases (82 G12C) and 290 controls, with non-significant divergence from controls in later stages (Fig. 2E, $P = 0.213$).

Figure 2D, E showed no significant difference in immunotherapy efficacy between KRAS G12C and other KRAS mutations, so we didn't further subdivide KRAS mutations. Both KRAS and control groups were analyzed separately based on mono or combination immunotherapy. The control group showed better PFS and OS with combination therapy (Fig. 2F: PFS $P < 0.001$, mPFS 10.6 vs. 3.6 months, HR 0.542; Fig. 2G: OS $P < 0.05$, mOS 46.0 vs. 9.0 months, HR 0.386). For the KRAS group, combination therapy survival curves were higher than monotherapy but not significantly (Fig. 2H: PFS $P = 0.085$, mPFS 5.7 vs. 4.4 months, HR 0.698; Fig. 2I: OS $P = 0.095$, mOS 39.5 vs. 10.1 months, HR 0.399). The trends were similar to controls, and the lack of significance might be due to the smaller KRAS combination therapy sample size.

Additionally, we also analyzed whether the predictive efficacy of TMB and PD-L1 for immunotherapy and found it was consistent across the two groups (Online Resource Fig. S1).

KRAS mutant NSCLC exhibits stronger acquired chemoresistance

We stimulated cells from both the KRAS mutant group and the wild-type group with a gradient of different concentrations of paclitaxel, carboplatin, and pemetrexed (Online Resource Fig. S2A–S2C), and cell proliferation experiments indicated no significant difference in the inhibition rates of these three chemotherapy drugs on the two groups. Clonogenic assays showed no significant difference in the clonogenic ability of the two groups of cells under

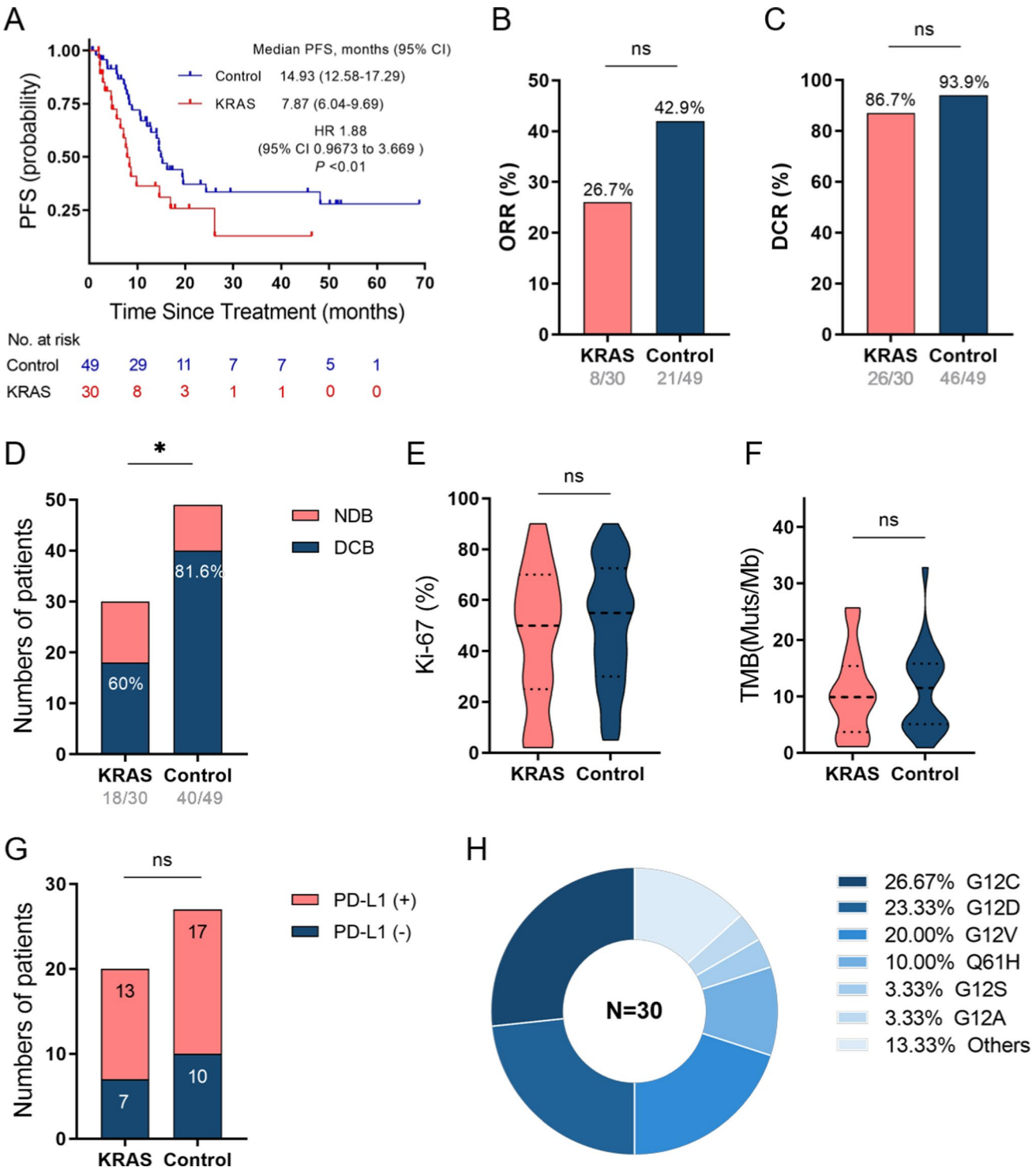

Fig. 1 First-line treatment efficacy and clinical features of KRAS mutant NSCLC. **A** PFS of first-line treatment in the KRAS group and the driver genes-negative group ($P < 0.05$, mPFS 7.87 VS 14.93 months, HR 1.88, 95% CI 0.9673–3.669); **B** ORR of the KRAS group and the driver genes-negative group; **C** DCR of the KRAS group and the driver genes-negative group; **D** DCB rates of the KRAS group and the driver genes-negative group; Ki-67 (**E**), TMB (**F**), and PD-L1 (**G**) expression of the KRAS and the control group; **H** mutant subtypes in the KRAS group

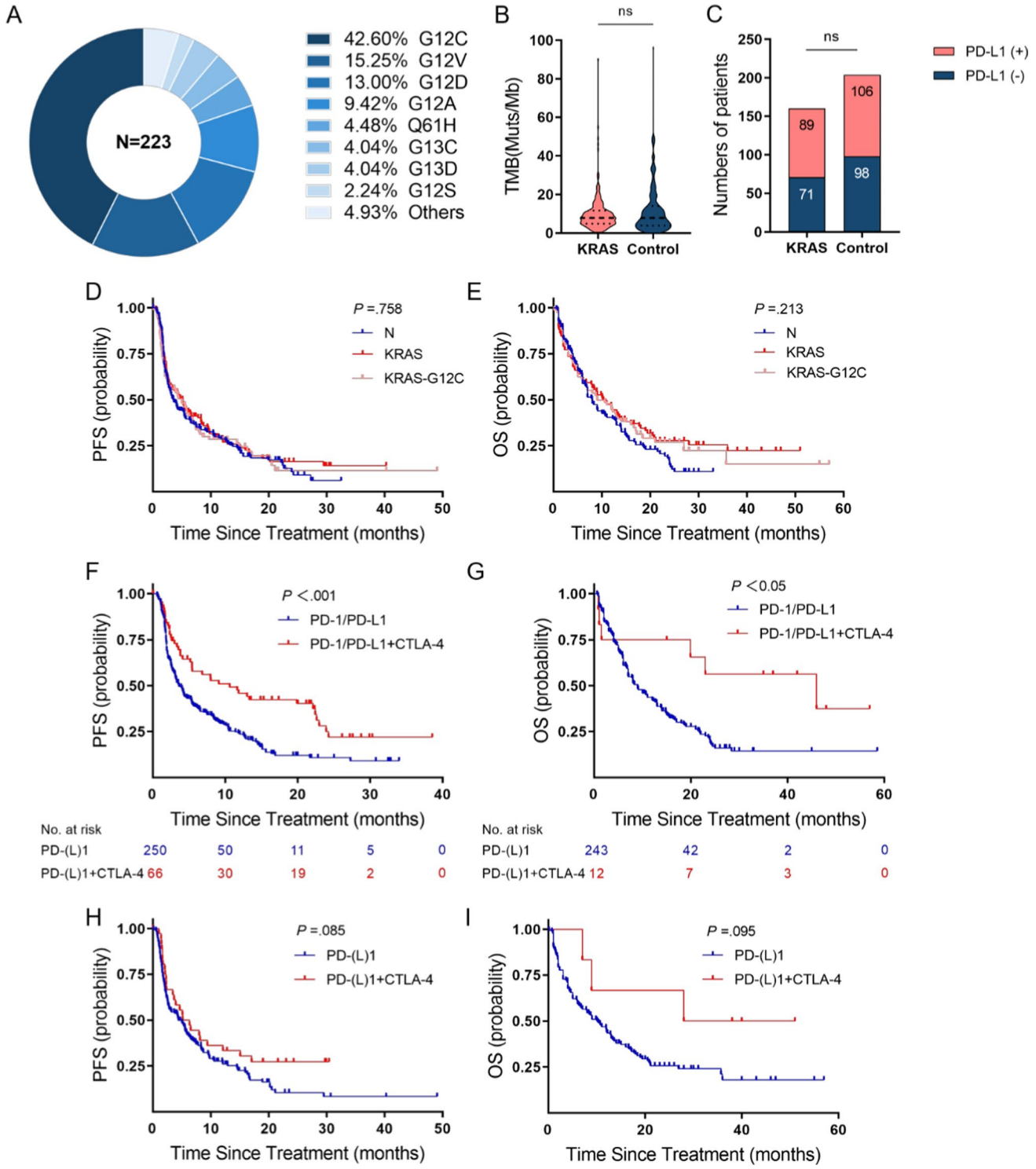

Fig. 2 Immunotherapy efficacy and clinical features of KRAS-mutant NSCLC. **A** Mutant subtypes in the KRAS group; **B** TMB expression of immunotherapy cases; **C** PD-L1 expression of immunotherapy cases; **D** PFS of immunotherapy in the KRAS G12C group (n = 95), the other KRAS mutations group (n = 128) and the driver genes-negative group (n = 316); **E** OS of immunotherapy in the KRAS G12C group (n = 82), the other KRAS mutations group (n = 112) and the driver genes-negative group (n = 290); **F** PFS of the driver genes-negative group with mono verses combined immunotherapy (mPFS 10.6 vs 3.6 months, HR 0.542, 95% CI 0.409–0.719); **G** OS of the driver genes-negative group with mono verses combined immunotherapy (mOS 46.0 vs 9.0 months, HR 0.386, 95% CI 0.227–0.657); **H** PFS of the KRAS group with mono verses combined immunotherapy (mPFS 5.7 vs 4.4 months, HR 0.698, 95% CI 0.481–1.011); **I** OS of the KRAS group with mono verses combined immunotherapy (mOS 39.5 vs 10.1 months, HR 0.399, 95% CI 0.189–0.843)

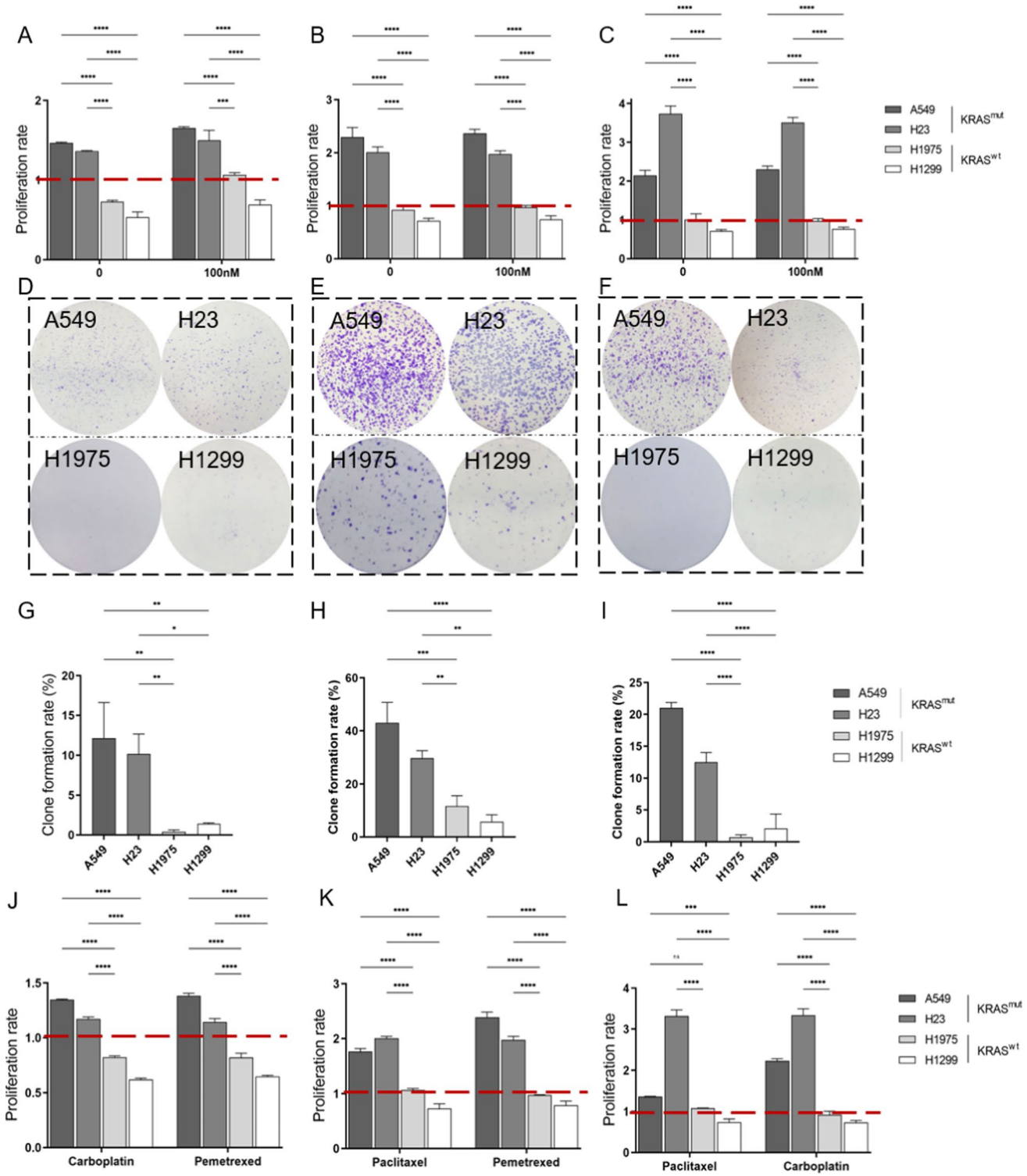
A
B
C
Proliferation rate
0
100nM
A549
H23
H1975
H1299
KRASmut
KRASwt
D
E
F
G
H
I
Clone formation rate (%)
J
K
L
Carboplatin
Pemetrexed
Paclitaxel

◂**Fig. 3** Proliferation and clonal changes of the KRAS mutant group and the wild-type group when treated with chemotherapy drugs. **A**–**C** Proliferation rate changes of the KRAS mutant group and the wild-type group when treated with paclitaxel (**A**), carboplatin (**B**), and pemetrexed (**C**) resistance models; **D**–**F** clone formation diagram of the KRAS-mutant group and the wild-type group when treated with paclitaxel (**D**), carboplatin (**E**), and pemetrexed (**F**) resistance models; **G**–**I** clone formation rate of the KRAS-mutant group and the wild-type group when treated with paclitaxel (**G**), carboplatin (**H**), and pemetrexed (**I**) resistance models; **J** proliferation rate changes of the KRAS mutant group and the wild-type group in carboplatin and pemetrexed after being treated with paclitaxel resistance models; **K** proliferation rate changes of the KRAS mutant group and the wild-type group in paclitaxel and pemetrexed after being treated with carboplatin resistance models; **L** proliferation rate changes of the KRAS mutant group and the wild-type group in paclitaxel and carboplatin after being treated with pemetrexed resistance models; Clone formation rate = (amount of clones/number of seeded cells) × 100%; Proliferation rate was calculated by dividing the cell viability in the drug pretreatment group by the cell viability in the control group. A ratio less than 1 means that cell proliferation activity decreases after drug stimulation, while a ratio greater than 1 indicates an increase in cell proliferation activity and the development of drug resistance. Variables were expressed as mean ± SEM, $^{*}P < 0.05$, $^{**}P < 0.01$, $^{***}P < 0.001$, $^{****}P < 0.0001$, ns: no significance; the experiment was repeated at least 3 times

non-intervention conditions (Online Resource Fig. S2D, S2E).

After treating the KRAS mutant group and wild-type group with the paclitaxel chemoresistance model, we found that the KRAS mutant group exhibited an increase in proliferation rate more quickly in the presence of paclitaxel (Fig. 3A), with a proliferation rate not only significantly higher than the wild-type group, but also greater than 1, indicating the development of chemoresistance to paclitaxel. Similarly, we repeated the above experiment using carboplatin and pemetrexed. Cells from the KRAS mutant group showed a quicker increase in proliferation rate in both carboplatin (Fig. 3B) and pemetrexed (Fig. 3C), with a proliferation rate not only significantly higher than the wild-type group but also greater than 1. Clonogenic assays showed that the KRAS mutant group had stronger clonogenic ability in paclitaxel (Fig. 3D, G), carboplatin (Fig. 3E, H), and pemetrexed (Fig. 3F, I).

These results above explained the lack of statistical significance in the differences of ORR and DCR between the KRAS group and the control group in the retrospective analysis, while the difference in the proportion of DCB is statistically significant. Compared to ORR and DCR, DCB places more emphasis on the duration of effective treatment in evaluating the efficacy.

Additionally, we found that the proliferation rate of KRAS mutant group cells treated with the paclitaxel chemoresistance model was also greater than 1 in carboplatin and pemetrexed (Fig. 3J), indicating that KRAS mutant NSCLC developed cross-resistance to carboplatin and pemetrexed after acquiring chemoresistance through paclitaxel stimulation. The same results were observed for the cross-resistance to carboplatin and pemetrexed; the KRAS mutant group treated with the carboplatin chemoresistance model showed a proliferation rate greater than 1 in paclitaxel and pemetrexed (Fig. 3K), and the KRAS mutant group treated with the pemetrexed chemoresistance model also showed a proliferation rate greater than 1 in paclitaxel and carboplatin (Fig. 3L).

The increase in proliferation rate of the KRAS mutant group in the three chemotherapy drugs—paclitaxel, carboplatin, and pemetrexed—indicates the formation of acquired chemoresistance, and the same increase in proliferation rate in the other two drugs after treatment with one drug suggests that this group of tumors has the ability to develop cross-resistance to different types of chemotherapy drugs. Therefore, we speculate that the chemoresistance of KRAS mutant NSCLC to chemotherapy is not specific but rather a non-specific chemoresistance formed through some common pathway downstream of KRAS mutation.

KRAS mutant NSCLC acquires adaptive chemoresistance through overexpression of SLC7A11

Given previous research showing that RAS-mutated cells have low expression of GPX4, and that the compounds RSL3 and Erastin have selective cytotoxicity to RAS-mutated cells by directly or indirectly inhibiting GPX4, we were interested in whether this selective cytotoxicity could be applied to the treatment of KRAS mutant NSCLC. Therefore, we treated KRAS mutant and wild-type NSCLC with the ferroptosis inducers RSL3 and Erastin (Online Resource Fig. S3A, S3B), but found that for KRAS mutant NSCLC, both compounds lost their selective toxicity.

By analyzing two TCGA datasets and five NSCLC-GSE datasets, we found that in KRAS mutant NSCLC, as shown in Online Resource Table S5 and Fig. S4, the correlation between KRAS and GPX4 expression was inconsistent across the datasets, while the expression levels of KRAS and SLC7A11 showed a positive correlation in all seven datasets.

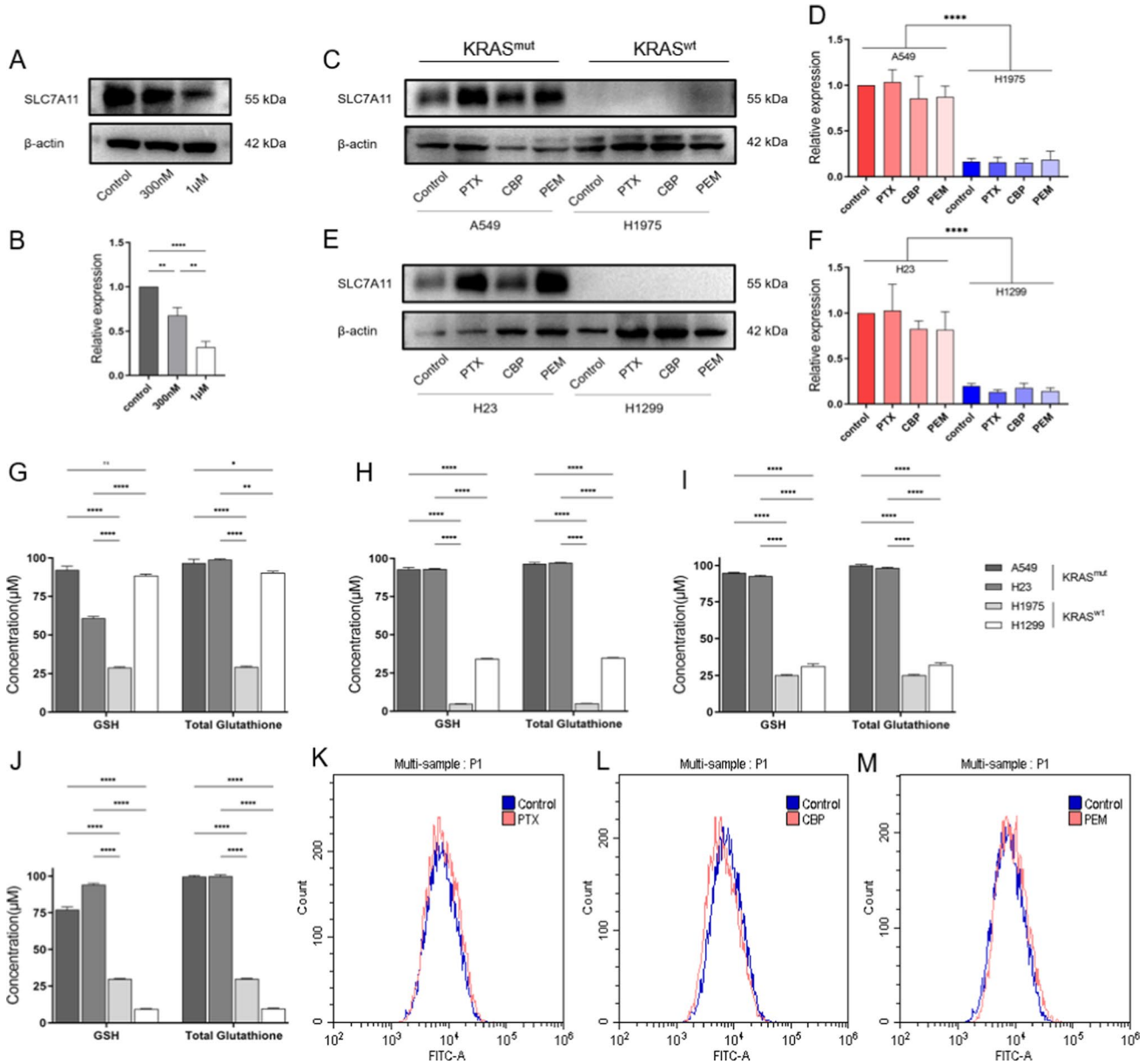

Fig. 4 KRAS-mutant NSCLC maintains lipid peroxidation stability through high expression SLC7A11. **A**, **B** In KRAS mutant NSCLC, AMG510 inhibits SLC7A11 protein expression; Relative expression: the SLC7A11/β-actin of the control sample was corrected to 1, and the expression levels in the other groups were all relative expressions compared with the control sample; **C**–**F** SLC7A11 expression before and after stimulating by chemotherapy drugs of the KRAS mutant group and the wild-type groups; relative expression: the SLC7A11/β-actin of the control sample in the KRAS mutant group was corrected to 1, and the other samples' expression levels were all relative expressions compared with the control sample in the KRAS mutant groups; changes in intracellular GSH and total glutathione content in KRAS mutant groups compared to wild-type groups before (**G**) and after stimulation with paclitaxel (**H**), carboplatin (I), and pemetrexed (**J**); KRAS mutant NSCLC cells maintain stable levels of lipid peroxidation before (**K**) and after stimulation with paclitaxel (**K**), carboplatin (**L**) and pemetrexed (**M**); PTX: paclitaxel; CBP: carboplatin; PEM: pemetrexed; Variables were expressed as mean ± SEM. The experiment was repeated at least 3 times

We treated the KRAS G12C mutant H23 with the KRAS G12C inhibitor AMG510, and WB indicated that AMG510 significantly reduced the expression of SLC7A11 (Fig. 4A, B), with the inhibition efficiency being positively correlated with the dose of AMG510—the higher the dose, the lower of SLC7A11 protein expression. That is to say, targeted KRAS drugs can indirectly inhibit SLC7A11 by suppressing KRAS mutations. Compared to the KRAS wild-type group, cells in the KRAS mutant group significantly overexpressed SLC7A11, and after stimulation with paclitaxel, carboplatin, and pemetrexed, SLC7A11 was still able to maintain high-level expression (Fig. 4C–F).

SLC7A11 is primarily responsible for transporting glutamine and cystine in cells, thereby regulating glutathione within the cell. The glutathione in cells includes GSH and Oxidized Glutathione (GSSG), with most of it in the GSH state. Therefore, we further measured GSH and total glutathione within these two groups of cells. As shown in Fig. 4G, the initial GSH content varied among the different groups of cells. After stimulation with the three chemotherapy drugs, paclitaxel (Fig. 4H), carboplatin (Fig. 4I), and pemetrexed (Fig. 4J), the KRAS mutant group was consistently able to maintain a higher intracellular GSH content.

As an important reducing agent within cells, GSH plays a crucial role in maintaining cellular redox homeostasis. Subsequently, we detected the changes of lipid peroxidation within KRAS mutant cells before and after exposure to chemotherapy drug stimulation. After stimulation with paclitaxel (Fig. 4K), carboplatin (Fig. 4L), and pemetrexed (Fig. 4M), the lipid peroxidation within KRAS mutant NSCLC cells remained stable.

KRAS mutant NSCLC may acquire adaptive drug resistance by overexpressing SLC7A11, which increases the intracellular GSH level and thereby reduces the oxidative stress damage caused by various external stimuli, giving the cells a stronger adaptive capacity. We speculate that this may be related to the acquired drug resistance ability of KRAS mutant NSCLC.

After comparing three different siRNA sequences, we selected the siRNA-2 sequence with the highest inhibition efficiency for subsequent experiments (Fig. 5A, B). When we suppressed SLC7A11, cell viability of KRAS mutant NSCLC was not affected (Fig. 5C). However, for KRAS mutant cells that had developed drug resistance, their proliferation rates in paclitaxel, carboplatin, and pemetrexed (Fig. 5D–F) significantly decreased, even lower than the rate before drug resistance was established (the relative proliferation rate was not only less than that of the control group but also less than 1), indicating that the KRAS mutant NSCLC, which had developed drug resistance, has regained sensitivity to chemotherapy drugs. At the same time, in the cross-drug resistance tests with the three drugs, paclitaxel, carboplatin, and pemetrexed (Fig. 5G–I), the proliferation rate of KRAS mutant NSCLC was not only lower than that of the control group but also less than 1, indicating that the cross-resistance of tumor cells also disappeared when SLC7A11 was inhibited.

After suppressing SLC7A11, we again detected the changes of lipid peroxidation in KRAS mutant NSCLC cells before and after exposure to chemotherapy stimulation. After stimulation with paclitaxel, carboplatin and pemetrexed (Fig. 5J–L), lipid peroxidation within KRAS mutant cells significantly increased.

In animal experiments, we divided the chemotherapy regimen into a paclitaxel group, a carboplatin combined with pemetrexed group. A group treated with the SLC7A11 inhibitor Erastin combined with chemotherapy was compared to the group treated with chemotherapy alone. Paclitaxel combined with Erastin (Fig. 6A) significantly inhibited tumor growth and also reduced Ki-67 within the tumor (Fig. 6B, C). The results of the carboplatin combined with pemetrexed regimen (Fig. 6D–F) were consistent with the paclitaxel. The Erastin combined with carboplatin and pemetrexed group showed a more significant inhibitory effect on tumor growth compared to the carboplatin combined with pemetrexed group alone, and Ki-67 in the Erastin combined with chemotherapy group was lower than that in the group of chemotherapy only.

Discussion

In the retrospective analysis, some patients also received antiangiogenic therapy or radiotherapy, but the COX multivariate analysis indicated that these parts of treatment had no significant impact in the two groups. We found no significant difference in immunotherapy efficacy between the KRAS mutant and the wild-type population, indicating that the KRAS mutation did not affect immunotherapy.

We discovered KRAS-mutant NSCLC can develop adaptive resistance to one chemo drug and cross-resistance to two others (paclitaxel, carboplatin, pemetrexed). This suggests a common KRAS mutation pathway, not drug-specific mechanisms, may be responsible. We considered ferroptosis inducers RSL3 and Erastin, known for their selective toxicity to RAS-mutated cells.

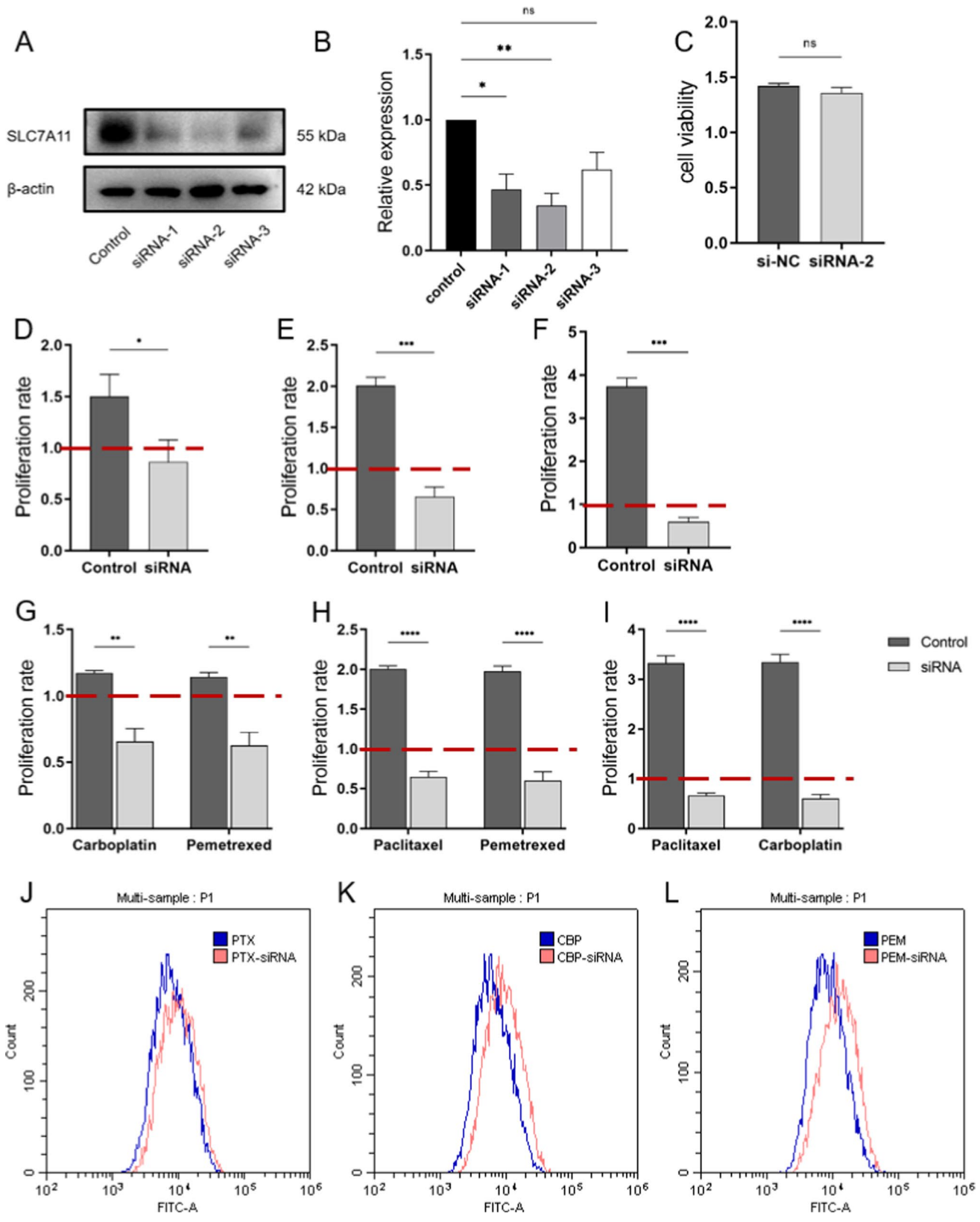
A
SLC7A11
55 kDa
β-actin
42 kDa
Control
siRNA-1
siRNA-2
siRNA-3
B
Relative expression
ns
**
*
control
siRNA-1
siRNA-2
siRNA-3
C
cell viability
ns
si-NC
siRNA-2
D
Proliferation rate
*
Control
siRNA
E
Proliferation rate
***
Control
siRNA
F
Proliferation rate
***
Control
siRNA
G
Proliferation rate
**
**
Carboplatin
Pemetrexed
H
Proliferation rate
****
****
Paclitaxel
Pemetrexed
I
Proliferation rate
****
****
Paclitaxel
Carboplatin
Control
siRNA
J
Multi-sample : P1
PTX
PTX-siRNA
Count
FITC-A
K
Multi-sample : P1
CBP
CBP-siRNA
Count
FITC-A
L
Multi-sample : P1
PEM
PEM-siRNA
Count
FITC-A

◂**Fig. 5** Inhibition of SLC7A11 expression restores the sensitivity of KRAS-mutant NSCLC to chemotherapy. **A**, **B** Inhibition efficiency of three siRNA sequences; **C** no significant change in cell proliferation viability after inhibiting SLC7A11; changes in proliferation rates of drug-resistant KRAS mutant NSCLC in paclitaxel (**D**), carboplatin (**E**), and pemetrexed (**F**) after inhibiting SLC7A11 expression; **G** proliferation rate changes of KRAS mutant cells treated with a paclitaxel-resistant model in carboplatin and pemetrexed after inhibiting SLC7A11 expression; **H** proliferation rate changes of KRAS mutant cells treated with a carboplatin-resistant model in paclitaxel and pemetrexed after inhibiting SLC7A11 expression; **I** proliferation rate changes of KRAS mutant cells treated with a pemetrexed-resistant model in paclitaxel and carboplatin after inhibiting SLC7A11 expression; **J**–**L** After the suppression of SLC7A11, lipid peroxidation within KRAS mutant NSCLC cells increased upon exposure to paclitaxel (**J**), carboplatin (**K**), and pemetrexed (**L**); relative expression: the control group SLC7A11/β-actin is normalized to 1, and the relative expression of other groups is relative to the control group; proliferation rate = cell vitality of the drug-pretreated group/cell vitality of the non-pretreated group. A ratio less than 1 indicates a decrease in cell vitality after drug stimulation (i.e., sensitivity to the drug), and a ratio greater than 1 indicates an increase in cell proliferation vitality after drug stimulation (i.e., development of drug resistance); PTX: paclitaxel; CBP: carboplatin; PEM: pemetrexed; in this figure, siRNA refers to sequence siRNA-2

Approximately 20% of KRAS mutant cells lack kelch-like-erythroid cell-derived protein with CNC homology (ECH)-associated-protein 1 (KEAP1) gene function. As KEAP1 is a negative regulator of the nuclear factor erythroid 2-related factor 2 (NRF2) nuclear factor, the loss of KEAP1 leads to the activation of NRF2. The expression of SLC7A11 is consistent with NRF2, and after suppressing NRF2, SLC7A11 is also partially reduced. Inhibitors of SLC7A11 can selectively kill KRAS mutant cells [13–15]. This may partially explain the principle of high expression of SLC7A11 in KRAS mutant tumor cells, but more mechanisms still need to be further explored. RSL3 and Erastin have been reported for their special selective cytotoxicity to RAS-mutated cells [11, 16], but our experiments and some literature suggest that in tumors, especially in NSCLC, whether it is SLC7A11 inhibitors or GPX4 inhibitors, they actually lose their specific toxicity to KRAS mutant cells when used alone [17]. The mechanism of the two compounds was mainly to directly or indirectly inhibit the relatively low expression of GPX4 in RAS-mutated cells, thereby achieving selective cytotoxicity at lower concentrations [11, 16]. However, KRAS mutant NSCLC's SLC7A11 overexpression compensates for low GPX4, enhancing survival. Even without selectivity, SLC7A11 inhibitors can overcome drug resistance in KRAS mutant NSCLC, offering new clinical treatment insights.

SLC7A11 is overexpressed in various tumors, not just KRAS mutant NSCLC. While this grant increased resistance to external stimuli, it also increases metabolic dependence on glucose and glutamine, offering a potential therapeutic target [18].

Our experiments indicated that inhibiting KRAS G12C could enhance chemo sensitivity by indirectly reducing SLC7A11, with greater effects at higher doses. This suggests potential for synergistic benefits from combined targeted and chemotherapy approaches in treating KRAS mutant NSCLC.

The role of the GSH axis is mainly to give cells a stronger adaptability to various external stimuli, including adaptability to various anti-tumor drugs. Whether KRAS mutant NSCLC has stronger metastatic and transfer capabilities compared to other types of lung cancer is still unknown, and more analysis is still needed to uncover related phenotypes.

This study was initiated by the question "Does KRAS mutation affect the efficacy of advanced NSCLC?" which arose from a few cases with poor efficacy of KRAS mutations encountered in clinical treatment. Through retrospective analysis, we expanded the population and found a clinical phenomenon where patients with KRAS mutations had poorer first-line treatment efficacy in advanced NSCLC compared to those without driver gene mutations. By further analyzing immunotherapy and chemotherapy separately, we ultimately found that KRAS-mutant non-small cell lung cancer can maintain its GSH levels through high expression of SLC7A11, thereby gaining stronger antioxidant stress capabilities and ultimately demonstrating acquired chemoresistance. This study has preliminarily resolved the initial question: KRAS mutations can affect treatment efficacy through stronger acquired chemoresistance. However, this study still has many shortcomings, such as a small sample size in the first part of the retrospective analysis and the concurrent use of antiangiogenic therapy in some patients. The exploration of mechanisms in this study is also relatively superficial. We hope to further expand the sample size in subsequent studies and conduct a more in-depth discussion of the molecular mechanisms involved.

Conclusion

Our research delves into the diminished efficacy of first-line immunotherapy combined with chemotherapy in advanced NSCLC with KRAS mutations, as compared to those without driver genes under identical treatment protocols. Through a detailed analysis of immunotherapy and chemotherapy within the KRAS-mutant NSCLC cohort, we reveal that the KRAS mutation itself does not impede the effectiveness of immunotherapy. Instead, it triggers an overexpression of SLC7A11, endowing the tumor with enhanced chemoresistance.

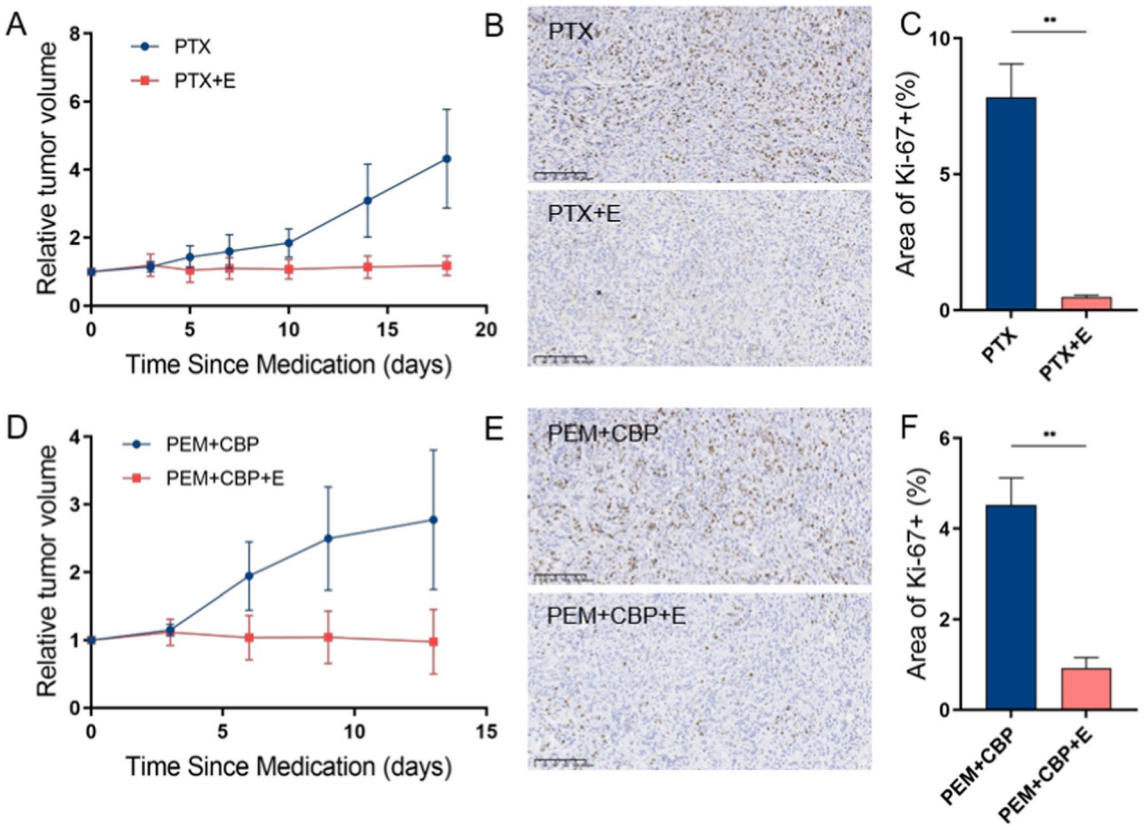

Fig. 6 Combination of Erastin with chemotherapy inhibits tumor growth compared to chemotherapy alone. **A** Tumor growth changes in the Erastin plus paclitaxel group compared to the paclitaxel alone group (relative tumor volume = volume on day × after treatment/volume before treatment); **B**, **C** comparison of Ki-67 expression levels in tumors between the Erastin plus paclitaxel group and the paclitaxel alone group (×10 magnification); **D** tumor growth changes in the Erastin plus pemetrexed and carboplatin group compared to the pemetrexed and carboplatin group; **E**, **F** comparison of Ki-67 expression levels in tumors between the Erastin plus pemetrexed and carboplatin group and the pemetrexed and carboplatin alone group (×10 magnification); *PTX* paclitaxel, *CBP* carboplatin, *PEM* pemetrexed

Supplementary Information The online version contains supplementary material available at https://doi.org/10.1007/s12094-024-03592-4.

Acknowledgements We are grateful for the collation and sharing of clinical information on the cBioPortal for Cancer Genomics website.

Funding This research was funded by the National Natural Science Foundation of China, Grant number 82172708.

Declarations

Conflict of interest The authors declare no conflicts of interest.

Ethnics statement The collection of data for the retrospective analysis was approved by the Ethics Committee of The First Affiliated Hospital with Nanjing Medical University (Number: 2022-SR-357). The animal experiments were approved by the Animal Core Facility of Nanjing Medical University (Number: IACUC-2201042).

References

1. Martin P, Leighl NB, Tsao MS, Shepherd FA. KRAS mutations as prognostic and predictive markers in non-small cell lung cancer. J Thorac Oncol. 2013;8:530–42.
2. Adderley H, Blackhall FH, Lindsay CR. KRAS-mutant non-small cell lung cancer: converging small molecules and immune checkpoint inhibition. EBioMedicine. 2019;41:711–6.
3. Collisson EA, Campbell JD, Brooks AN, Berger AH, Lee W, Chmielecki J, et al. Comprehensive molecular profiling of lung adenocarcinoma. Nature. 2014;511:543–50.
4. Chen X, Kang R, Kroemer G, Tang D. Broadening horizons: the role of ferroptosis in cancer. Nat Rev Clin Oncol. 2021;18:280–96.
5. Johnson L, Mercer K, Greenbaum D, Bronson RT, Crowley D, Tuveson DA, et al. Somatic activation of the K-ras oncogene causes early onset lung cancer in mice. Nature. 2001;410:1111–6.
6. Rodenhuis S, Slebos RJC. The ras oncogenes in human lung cancer. Am Rev Respir Dis. 1990. https://doi.org/10.1164/AJRCCM/142.6_PT_2.S27.
7. Bansal A, Celeste Simon M. Glutathione metabolism in cancer progression and treatment resistance. J Cell Biol. 2018;217:2291–8.

8. Nakajima EC, Ren Y, Vallejo JJ, Akinboro O, Mishra-Kalyani PS, Larkins EA, et al. Outcomes of first-line immune checkpoint inhibitors with or without chemotherapy according to KRAS mutational status and PD-L1 expression in patients with advanced NSCLC: FDA pooled analysis. J Clin Oncol. 2022;40:9001–9001. https://doi.org/10.1200/JCO.2022.40.16_suppl.9001.
9. Yang WS, Sriramaratnam R, Welsch ME, Shimada K, Skouta R, Viswanathan VS, et al. Regulation of ferroptotic cancer cell death by GPX4. Cell. 2014;156:317–31.
10. Tang D, Chen X, Kang R, Kroemer G. Ferroptosis: molecular mechanisms and health implications. Cell Res. 2021;31:107–25.
11. Dixon SJ, Lemberg KM, Lamprecht MR, Skouta R, Zaitsev EM, Gleason CE, et al. Ferroptosis: an iron-dependent form of nonapoptotic cell death. Cell. 2012;149:1060–72.
12. Niu B, Liao K, Zhou Y, Wen T, Quan G, Pan X, et al. Application of glutathione depletion in cancer therapy: enhanced ROS-based therapy, ferroptosis, and chemotherapy. Biomaterials. 2021. https://doi.org/10.1016/J.BIOMATERIALS.2021.121110.
13. Hu K, Li K, Lv J, Feng J, Chen J, Wu H, et al. Suppression of the SLC7A11/glutathione axis causes synthetic lethality in KRAS-mutant lung adenocarcinoma. J Clin Investig. 2020;130:1752–66.
14. Xu Y, Li Y, Li J, Chen W. Ethyl carbamate triggers ferroptosis in liver through inhibiting GSH synthesis and suppressing Nrf2 activation. Redox Biol. 2022. https://doi.org/10.1016/J.REDOX.2022.102349.
15. Wang X, Chen X, Zhou W, Men H, Bao T, Sun Y, et al. Ferroptosis is essential for diabetic cardiomyopathy and is prevented by sulforaphane via AMPK/NRF2 pathways. Acta Pharm Sin B. 2022;12:708–22.
16. Dolma S, Lessnick SL, Hahn WC, Stockwell BR. Identification of genotype-selective antitumor agents using synthetic lethal chemical screening in engineered human tumor cells. Cancer Cell. 2003;3:285–96.
17. Xu T, Ding W, Ji X, Ao X, Liu Y, Yu W, et al. Molecular mechanisms of ferroptosis and its role in cancer therapy. J Cell Mol Med. 2019;23:4900–12.
18. Liu X, Nie L, Zhang Y, Yan Y, Wang C, Colic M, et al. Actin cytoskeleton vulnerability to disulfide stress mediates disulfidptosis. Nat Cell Biol. 2023;25:404–14.